LargeBRAT! Complex Backward Reach-Avoid Tubes: An Emergent Collective Behavior Perspective.

Olalekan Ogunmolu[*] and Sylvia Herbert[†]

[*]Microsoft Research, NYC, 300 Lafayette Street, New York, NY 10012, USA
[†]UC San Diego, La Jolla, CA, USA.
lekanmolu@microsoft.com, sherbert@eng.ucsd.edu.

Abstract. Whereas until now, the numerical verification of *complex* and *nonlinear* systems via the Isaacs equation (with an overapproximation guarantee of the reachable set or tube) has proven elusive owing to the exponential computational complexity associated with resolving value functions on a mesh. In this work, we present a globally isotropic yet locally anisotropic reachable set/tube computational scheme, that enables the computation of the reach-avoid-tubes of multiple agents interacting over a large state space by exploiting the resolution of the extrema of payoffs on local substructures of the state space whilst preserving desirable global payoff properties. Within the bounds here set, our scheme presents a simple yet effective strategy for designing the verification of *nonlinear systems* for large backward reach-avoid sets or tubes.

1 INTRODUCTION.

Cyberphysical systems (or CPS) are a complex network of control systems, their actuators, sensing mechanisms, and software whose communication protocols involve a complex labyrinth of interactions that may be difficult to analyze or synthesize with closed-form analytical propositions. Finding stable, optimal and robust control laws in the presence of complex dynamics with convergence guarantees; planning and low-level control in real-time collision avoidance scenarios in uneven terrains, or sensing efficiently in the presence of multiple agents – all require active control, and a deep integration of the actions of system components. Therefore, the control of combined CPS systems in the presence of sensing, control, and learning constraints becomes timely and crucial. Differential optimal control theory and games offer a useful paradigm for resolving the safety of multiple agents interacting over a shared space. Both rely on the resolution of the Hamilton-Jacobi-Bellman (HJB) or the Hamilton-Jacobi-Isaacs (HJI) equation.

As HJ-type equations have no classical solution for almost all *practical* problems, stable numerical and computational methods need to be brought to bear in order to produce solutions with (approximately) optimal guarantees. With essentially non-oscillating (ENO) [1] Lax-Friedrichs [2] schemes applied to numerically resolve HJ Hamiltonians [3], we can now obtain *consistent* and *monotone* (viscosity) solutions to HJ-type equations[1] with high accuracy and precision *on a mesh*. However, resolving HJI solutions

---

[1] By consistency, we mean that the numerical approximation to (Cauchy-type) HJ equations agree with the initial value problem; and by monotone schemes, we mean that the explicit
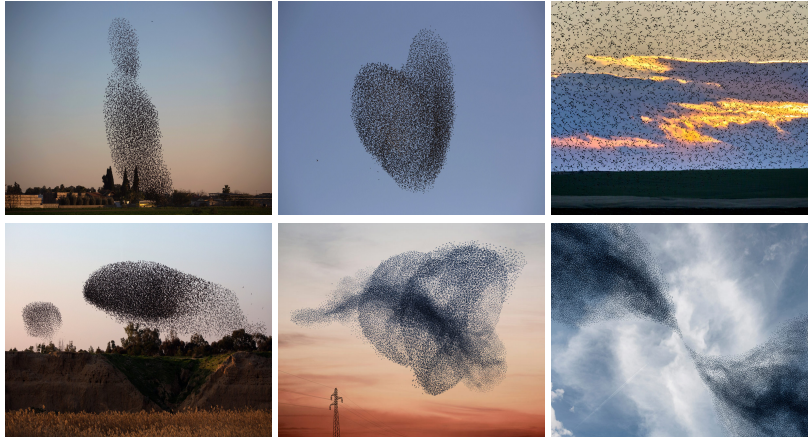
Fig. 1: Starlings murmurations. From the top-left and clockwise. (i) A starlings flock rises into the air, in an anisotropical and dense structure (Reuters/Amir Cohen). (ii) Starlings migrating over an Israeli Village (AP Photo/Oded Balilty). (iii) Starlings feeding on the seeds already laid in the ground in Romania. (iv) Two flocks of migrating starlings (Menahem Kahana/AFP/Getty Images). (v) A concentric conical dense formation of starlings (Courtesy of The Gathering Site.). (vi) Splitting and joining of a flock.
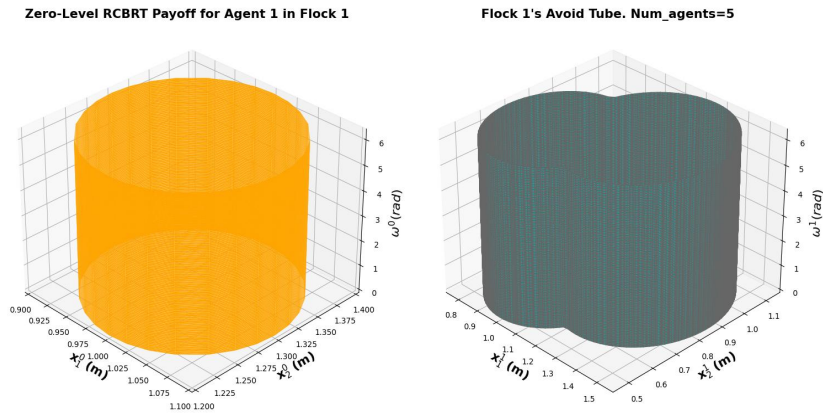

Fig. 2: Left: Initial zero level RCBRT of a single agent's payoff within a flock. Right: Union of the zero-level RCBRT of all agents within a flock. This is the local backward avoid tube for this flock. For as many local flocks as are in a murmuration, collision avoidance is maintained by taking the respective unions of individual flock's RCBRTs.

on a mesh is not scalable [5–7] owing to the curse of dimensionality [8], as the value function is resolved on a dimension-by-dimension basis on a grid.

_____

marching schemes which are a nondecreasing function of each argument of the vector field upon which the state is defined. For more details, see [4].

Through empirical [11–13] and theoretical findings [14], evidence now abounds that in certain natural species that exhibit collective behavior (see Fig. 1), convergence and group cohesion is based on simple topological interaction rules that they use to keep a tab on one another in *local flocks* for collision avoidance, preserving density and structure, flock splitting, vacuole, cordon, and flash expansion [15]. This helps these animals preserve an eye-pleasing local anisotropic synchrony, which taken together among possibly hundreds of thousands of local interactions[2] [15], keep these animals whirling, swooping, and flying in an isotropic formation [11].

Individual agents aggregate into finite flocks, and flock motion is synergized via local topological interactions in order to realize a stable global heading and cohesion [14]. There exists limited evidence that when an agent within a flock of starlings senses danger (e.g. an attack from a Peregrine Falcon), it changes its course immediately. Owing to the lateral vision in such animals, immediate *nearest neighbors* change course in response. This information is propagated across the entire group of flocks within the fraction of a second, resulting in the wondrous formation and observations that we see in the sky [11].

Local flocks maintain an anisotropic formation, regardless of sparsity of birds within a flock, which enables the entire collection of flocks to maintain an isotropic formation owing to these simple topological interactions. Thus, collision is avoided, attacks are fended off, and there is a conjecture that the birds keep warm in winter when they exercise these behaviors before traveling to their roosting site.

1.1 Collective Behavior From Local Objectives

Our goal here is the verification of *complex* and *nonlinear* behavior of *multi-agent autonomous systems* that is robust against a worst-case disturbance, and preserves local safety objectives *under global cohesion goals*. We draw inspiration from movement of animal groups with an emphasis on emergent complex behaviors via local interactions. Compelling evidence suggests that by observing local anisotropic formation behaviors [11], collective behaviors emerge which helps maintain global isotropic behaviors that preserve unique formation patterns and group cohesion.

Seeing that these animals are able to generate emergent complex behaviors from local adaptive interactions with their nearest neighbors, we find it compelling to draw inspiration from these collective interactions. To analyze safety, we formulate the problem within *Cauchy-type* HJ problems [16], and we resolve the differential optimal control [17] problem within the *robustly backward reachable tube* scheme of [9]. Our focus is verifying complex cohesion behaviors in multi-agent dynamical systems, interacting over a large state space, while mitigating against the computational complexity associated with computing large backward reach-avoid-tubes(BRATs) [5, 7, 18]. While the inspiration for this verification work draws from Mitchell's body of work [10], we broaden the definition of target sets and system dynamics from basic Dubins' scheme formulations to consensus headings of vehicular dynamics under topological nearest neighbor rules in manifolds of the state space.

---

[2] It has been reported that no birds fly together with greater coordination and complexity as European starlings, with murmurations counting upwards of 750,000 individual birds!

While Jadbabaie et al. [14] introduced a graphical formulation based on a switched linear system to demonstrate that nearest neighbor rules cause agents to converge to the same heading, we stick with the nonlinear model of the system and employ *reachability analysis* as a tool. We introduce new insights, and computational techniques aimed at solving *practical* problems that cannot be otherwise analytically resolved nor numerically resolved without exploiting state substructures and parallelism. This work is the first to systematically provide a rational separated value function aggregation scheme on local grids in computing RCBRTs for large state spaces.

The rest of this paper is organized as follows: we introduce common notations and definitions in § 2; § 3 describes the concepts and topics we will build upon in describing our proposal in § 4; we present results and insights from experiments in **??**. We conclude the paper in § 6.

2   Notations and Definitions.

Let us now introduce the notations that are commonly used in this article. Time variables e.g. t, t_0, τ, T will always be real numbers. We let $t_0 \leq t \leq t_f$ denote fixed, ordered values of t. Vectors shall be column-wise stacked and be denoted by small bold-face letters i.e. $\mathbf{e}, \mathbf{u}, \mathbf{v}$ e.t.c. Matrices will be denoted by bold-math Latin upper case fonts e.g. $\mathbf{T}, \mathbf{S}$. Exceptions: the unit matrix is I; and i, j, k are indices. We adopt zero-indexing for matrix operations throughout so that if index i corresponds to size I, we shall write $i = 0, 1, \cdots, I - 1$. Positive, negative, decreasing, increasing e.t.c. shall refer to strict corresponding property.

2.1   Sets, Controls, and Games.

The set S of all $\boldsymbol{x}$ such that $\boldsymbol{x}$ belongs to the real numbers $\mathbb{R}$, and that $\boldsymbol{x}$ is positive shall be written as $S = \{\boldsymbol{x} \,|\, \boldsymbol{x} \in \mathbb{R}, \boldsymbol{x} > 0\}$. We define Ω as the open set in $\mathbb{R}^n$. To avoid the cumbersome phrase "the state $\boldsymbol{x}$ at time t", we will associate the pair $(\boldsymbol{x}, t)$ with the *phase* of the system for a state $\boldsymbol{x}$ at time t. Furthermore, we associate the Cartesian product of Ω and the space $T = \mathbb{R}^1$ of all time values as the *phase space* of $\Omega \times T$. The interior of Ω is denoted by $\text{int } \Omega$; whilst the closure of Ω is denoted $\bar{\Omega}$. We denote by $\delta\Omega \, (:= \bar{\Omega} \backslash \text{int } \Omega)$ the boundary of the set Ω.

Unless otherwise stated, vectors $\boldsymbol{u}(t)$ and $\boldsymbol{v}(t)$ are reserved for admissible control (resp. disturbance) at time t. We say $\boldsymbol{u}(t)$ (resp. $\boldsymbol{v}(t)$) is piecewise continuous in t, if for each t, $\boldsymbol{u} \in \mathcal{U}$ (resp. $\boldsymbol{v} \in \mathcal{V}$), $\mathcal{U}$(resp. $\mathcal{V}$) is a Lebesgue measurable and compact set. At all times, any of $\boldsymbol{u}$ or $\boldsymbol{v}$ will be under the influence of a *player* such that the motion of a state $\boldsymbol{x}$ will be influenced by the will of that player. Our theater of operations is that of conflicting objectives between a collection of agents with a heading convergence objective and an external disturbance. For agents that are members of a local coordination group, collision avoidance shall apply so that agents within a local neighborhood cooperate to avoid predators. Thus, the problem at hand assumes that of a pursuit *game*. And by a game, we do not necessarily refer to a single game, but rather a *collection of games*. Such a game will terminate when *capture* occurs, that is the distance between players falls below a predetermined threshold.

Each player in a game will constitute either a pursuer (P) or an evader (E). The cursory reader should not interpret P or E as controlling a single agent. In complex settings, we may have several pursuers (enemies) or evaders (peaceful citizens). However, when P or E governs the behavior of but one agent, these symbols will denote the agents themselves. The game shall terminate when a *capture* occurs, and when the distance between $|PE|$ becomes less than a threshold, we shall have a *capture*. Given the various possibilities of outcomes, the question of what is "best" will be resolved by a *payoff*, whose minimization, maximization, or an alternating best response min-max will constitute a *value function*, V. We adopt Isaac's [19] language so that if the payoff for a game is finite, we shall have a *game of kind*; and for a game with a continuum of payoffs, we shall have *a game of degree*. The strategy executed by P or E during a game shall be denoted by $\mathcal{A}$ (resp. $\mathcal{B}$). With this definition, a control law e.g. $u^{(i)}$ played by a player e.g. P will affect *agent* i; and a collection of agents under P's *willpower* be referred to as a flock. We shall refer to an aggregation of flocks on a state space as a *murmuration* [3].

3   Backward Reachability for Systems Verification.

A basic characteristic of a control system is to determine the point sets within the state space that are *reachable* with a control input choice. An example objective in *reachability analysis* could be a target ($\mathcal{L}$) protection objective by an evading player, E, from a pursuing player P. Our treatment here is a special case of Isaac's homicidal chauffeur's game [19], whereupon a P and E travel at a constant linear speeds, e.g. where the P seeks to drive an evader, E, into a target (or target set/tube), $\mathcal{L}$. When resolving the outcome of the game, a notion of *payoffs* is used. The payoff could be the distance from the target to the point/region of capture.

Backward reachability consists in avoiding an unsafe set of states under the worst-possible disturbance and at all times. The verification problem may consist in finding a *set of reachable states* that lie along the trajectories of the solution to a first order nonlinear P.D.E. that originates from some initial state $x_0 = x(0)$ up to a specified time bound, $t = t_f$. *From a set of initial and unsafe state sets, and a time bound, the time-bounded safety verification problem is to determine if there is an initial state and a time within the bound that the solution to the P.D.E. enters the unsafe set*.

Backward reachable sets (BRS) or tubes (BRTs) are popularly analyzed as a game of two vehicles with non-stochastic dynamics [20]. Such BRTs possess discontinuity at cross-over points (which exist at edges) on the surface of the tube, and may be non-convex. Mitchell's construction [10] does not necessarily use a state feedback control law during games and the worst-possible disturbance assumption is not formally inculcated in the backward reachability analyses used. In a sense, it is reasonable to ignore nonlinear robust control (e.g. $\mathcal{H}_\infty$) analyses for Dubins vehicles [21] with constant inputs that only vary in sign for either player [20] since the worst possible disturbance is known ahead of the game. In realistic problems, one may leverage an $\mathcal{H}_\infty$ scheme [22]'s in constructing an appropriate *worst-possible* disturbance that guarantees robustness in continuous control applications. We leave this to a future work.

---

[3] The definition of murmurations we use here has a semblance to the murmurations of possibly thousands of starlings observed in nature.

3.1   Reachability from Differential Games Optimal Control

In general, we seek for a *terminal payoff* $g(\cdot) : \mathbb{R}^n \to \mathbb{R}$ to satisfy

$$|g(\boldsymbol{x})| \leq k, \quad |g(\boldsymbol{x}) - g(\hat{\boldsymbol{x}})| \leq k|\boldsymbol{x} - \hat{\boldsymbol{x}}| \tag{1a}$$

for constant k and all $T \leq t \leq 0$, $\hat{\boldsymbol{x}}$, $\boldsymbol{x} \in \mathbb{R}^n$, $\boldsymbol{u} \in \mathcal{U}$ and $\boldsymbol{v} \in \mathcal{V}$. The zero sublevel set of $g(\boldsymbol{x})$ is

$$\mathcal{L}_0 = \{\boldsymbol{x} \in \bar{\Omega} \,|\, g(\boldsymbol{x}) \leq 0\}. \tag{2}$$

Suppose that the pursuer's mapping strategy (starting at t) is $\beta : \bar{\mathcal{U}}(t) \to \bar{\mathcal{V}}(t)$ provided for each $t \leq \tau \leq T$ and $\boldsymbol{u}, \hat{\boldsymbol{u}} \in \bar{\mathcal{U}}(t)$; then $\boldsymbol{u}(\bar{t}) = \hat{\boldsymbol{u}}(\bar{t})$ a.e. on $t \leq \bar{t} \leq \tau$ implies $\beta[\boldsymbol{u}](\bar{t}) = \beta[\hat{\boldsymbol{u}}](\bar{t})$ a.e. on $t \leq \bar{t} \leq \tau$. The player $\boldsymbol{P}$ is controlling β and minimizing, while the player $\boldsymbol{E}$ is controlling its strategy, α, and maximizing. The differential game's lower value for a solution $\boldsymbol{x}(t)$ that solves (7) for $\boldsymbol{u}(t)$ and $\boldsymbol{v}(t) = \beta[\boldsymbol{u}](\cdot)$ is

$$\boldsymbol{V}^-(\boldsymbol{x}, t) = \inf_{\beta \in \mathcal{B}(t)} \sup_{\boldsymbol{u} \in \mathcal{U}(t)} \boldsymbol{P}(\boldsymbol{u}, \beta[\boldsymbol{u}])$$

$$= \inf_{\beta \in \mathcal{B}(t)} \sup_{\boldsymbol{u} \in \mathcal{U}(t)} \int_t^T l(\tau, \boldsymbol{x}(\tau), \boldsymbol{u}(\tau), \beta[\boldsymbol{u}](\tau))d\tau + g(\boldsymbol{x}(T)). \tag{3}$$

We now establish the following Lemma from [23] that will aid the construction of the *robustly controlled backward reachable tube* – our main emphasis in this paper.

Lemma 1. *The lower value $\boldsymbol{V}^-$ of a differential game's terminal cost problem is the viscosity solution to the lower Isaac's equation*

$$\frac{\partial \boldsymbol{V}^-}{\partial t} + \boldsymbol{H}^-(t; \boldsymbol{x}, \boldsymbol{u}, \boldsymbol{v}, \boldsymbol{V}_{\boldsymbol{x}}^-) = 0, \ t \in [0, T] \ \boldsymbol{x} \in \mathbb{R}^n \tag{4a}$$

$$\boldsymbol{V}^-(\boldsymbol{x}, T) = g(x(T)), \quad \boldsymbol{x} \in \mathbb{R}^m \tag{4b}$$

with lower Hamiltonian,

$$\boldsymbol{H}^-(t; \boldsymbol{x}, \boldsymbol{u}, \boldsymbol{v}, p) = \max_{u \in \mathcal{U}} \min_{v \in \mathcal{V}} \langle f(t; \boldsymbol{x}, \boldsymbol{u}, \boldsymbol{v}), p \rangle. \tag{5}$$

where p, the co-state, is the spatial derivative of $\boldsymbol{V}^-$ w.r.t $\boldsymbol{x}$.

Proof. This lemma is an adaptation of [23, Th 4.1]. □

For any admissible control-disturbance pair $(\boldsymbol{u}(\cdot), \boldsymbol{v}(\cdot))$ and initial phase $(\boldsymbol{x}_0, t_0)$, Crandall [16] and Evan's [3] claim is that there exists a unique function

$$\boldsymbol{\xi}(t) = \boldsymbol{\xi}(t; t_0, \boldsymbol{x}_0, \boldsymbol{u}(\cdot), \boldsymbol{v}(\cdot)) \tag{6}$$

that satisfies

$$\dot{\boldsymbol{x}}(\tau) = f(\tau, \boldsymbol{x}(\tau), \boldsymbol{u}(\tau), \boldsymbol{v}(\tau)) \quad T \leq \tau \leq t, \quad \boldsymbol{x}(t) = \boldsymbol{x}, \tag{7a}$$

where $f(\tau, \cdot, \cdot, \cdot)$ and $\boldsymbol{x}(\cdot)$ are bounded and Lipschitz continuous. This bounded Lipschitz continuity property assures uniqueness of the system response $\boldsymbol{x}(\cdot)$ to controls $\boldsymbol{u}(\cdot)$ and $\boldsymbol{v}(\cdot)$ [23]. a.e. with the property that

$$\boldsymbol{\xi}(t_0) = \boldsymbol{\xi}(t_0; t_0, \boldsymbol{x}_0, \boldsymbol{u}(\cdot), \boldsymbol{v}(\cdot)) = \boldsymbol{x}_0. \tag{8}$$

Read (6): the motion of (7) passing through phase $(\boldsymbol{x}_0, t_0)$ under the action of control $\boldsymbol{u}$, and disturbance $\boldsymbol{v}$, and observed at a time t afterwards. One way to design a system verification problem is compute the reachable set of states that lie along the trajectory (6) such that we evade the unsafe sets up to a time e.g. t_f within a given time bound e.g. $[t_0, t_f]$. In this regard, we discard the HJ Cauchy-type P.D.E.'s *cost-to-go* [3] and certify safety as resolving a terminal value, $g(\boldsymbol{x}(T))$ at time T.

In backward reachability analysis, the lower value of the differential game [23] is used in constructing an analysis of the backward reachable set (or tube). Therefore, we can cast a target set as the time-resolved terminal value $\boldsymbol{V}^-(\boldsymbol{x}, T) = g(\boldsymbol{x}(T))$ so that given a time bound, and an unsafe set of states, the time-bounded safety verification problem consists in certifying that there is no phase within the target set (9) such that the solution to (7) enters the unsafe set. Following the backward reachability formulation of [10], we say the zero sublevel set of $g(\cdot)$ in (4) i.e.

$$\mathcal{L}_0 = \{\boldsymbol{x} \in \bar{\Omega} \mid g(\boldsymbol{x}) \leq 0\}, \tag{9}$$

is the *target set* in the phase space $\Omega \times \mathbb{R}$ for a backward reachability problem (proof in [10]). This target set can represent the failure set, regions of danger, or obstacles to be avoided etc in the state space. Note that the target set, $\mathcal{L}_0$, is a closed subset of $\mathbb{R}^n$ and is in the closure of Ω. And the *robustly controlled backward reachable tube* for $\tau \in [-T, 0]^4$ is the closure of the open set

$$\mathcal{L}([\tau, 0], \mathcal{L}_0) = \{\boldsymbol{x} \in \Omega \mid \exists \beta \in \bar{\mathcal{V}}(t) \, \forall \boldsymbol{u} \in \mathcal{U}(t), \exists \bar{t} \in [-T, 0],$$
$$\boldsymbol{\xi}(\bar{t}) \in \mathcal{L}_0\}, \bar{t} \in [-T, 0]. \tag{10}$$

Read: the set of states from which the strategies β of $\boldsymbol{P}$, and for all controls $\mathcal{U}(t)$ of $\boldsymbol{E}$ imply that we reach the target set within the interval $[-T, 0]$. More specifically, following Lemma 2 of [10], the states in the reachable set admit the following properties w.r.t the value function $\boldsymbol{V}$

$$\boldsymbol{x} \in \mathcal{L}_0 \implies \boldsymbol{V}^-(\boldsymbol{x}, t) \leq 0 \text{ and } \boldsymbol{V}^-(\boldsymbol{x}, t) \leq 0 \qquad \implies \boldsymbol{x} \in \mathcal{L}_0. \tag{11}$$

Observe:

- The goal of the pursuer, or $\boldsymbol{P}$, is to drive the system's trajectories into the unsafe set i.e., $\boldsymbol{P}$ has $\boldsymbol{u}$ at will and aims to minimize the termination time of the game (c.f. (9));
- The evader, or $\boldsymbol{E}$, seeks to avoid the unsafe set i.e., $\boldsymbol{E}$ has controls $\boldsymbol{v}$ at will and seeks to maximize the termination time of the game (c.f. (9));
- $\boldsymbol{E}$ has regular controls, $\boldsymbol{u}$, drawn from a Lebesgue measurable set, $\mathcal{U}$ (c.f. (3));

---

[4] The (backward) horizon, $-T$ is negative for $T > 0$.

- **P** possesses *nonanticipative strategies* (c.f. (3)) i.e. $\beta[\boldsymbol{u}](\cdot)$ such that for any of the ordinary controls, $\boldsymbol{u}(\cdot) \in \mathcal{U}$ of **E**, **P** knows how to optimally respond to **E**'s inputs.

This is a classic reachability problem on the resolution of the infimum-supremum over the *strategies* of **P** and *controls* of **E** with the time of capture resolved as an extremum of a cost functional) over a time interval i.e.

$$\frac{\partial \boldsymbol{V}^{-}}{\partial t}(\boldsymbol{x}, t) + \min\{0, \boldsymbol{H}^{-}(t; \boldsymbol{x}, \boldsymbol{u}, \boldsymbol{v}, \boldsymbol{V}_{\boldsymbol{x}}^{-})\} = 0 \tag{12a}$$

$$\boldsymbol{V}^{-}(\boldsymbol{x}, 0) = g(\boldsymbol{x}), \tag{12b}$$

where the vector field $\boldsymbol{V}_{\boldsymbol{x}}^{-}$ is known in terms of the game's terminal conditions so that the overall game is akin to a two-point boundary-value problem. Henceforward, for ease of readability, we will remove the minus superscript on the lower value and Hamiltonian (5).

4   Materials and Methods.

We cast the heading verification problem within a backward reachability analysis, where each agent within a flock have their respective payoff. Agents within a flock maintain cohesion by keeping track of their nearest neighbors' topological distance [11]. Capture occurs when an agent j is on or within a circular bound (specified by a radius, r in topological coordinates) around an agent i. To avoid capture, flocks can dynamically split their value functions. The value functions can be stitched together under a smoothness of boundaries assumption (as is observed in natural swarms) in order to fend off attacks from a pursuing player as well as manage the computation of a large RCBRT verification problem.

We synthesize the kinematics of agents that interact on distinct separate manifolds of the state space. These manifolds are called flocks in our description[5]. For each flock, there corresponds local value functions that encode a desirable anisotropic density and structural patterns we would like to emerge. These local value functions are constructed by taking into cognizance each agent's topological interaction rule with its neighbors [11]. By solving for these respective value functions simultaneously and in parallel, we can stitch them together at the end of each integration step by considering the nature of the *surfaces*[6] of the value functions at the end of each integration step. These simple tricks allows us to compute large backward reach-avoid tubes that have eluded other scalability methods that have been so far introduced [5, 18, 24].

Assumptions: The many interacting subsystems under consideration employ (i) natural units of measurements that are the same for all agents; (ii) kinematics with linear speeds but with a capacity for orientation changes; (iii) intra-flock agent interaction is restricted within unique and distinct state space manifolds; and by agents maneuvering their direction, a kinematic alignment is obtained; (iv) inter-flock interaction occurs

---

[5] Let the reader understand that we use the concept of a flock loosely. The value function could represent the cost of any large-scale control problem.

[6] Surfaces can be singular, dispersal, or universal in nature [19].

when a pursuer is within a threshold of capturing any agent within the murmuration. Let us now formalize definitions that will aid the modularization of the problem into manageable forms.

Definition 1. *We define a flock, F, of agents labeled $\{1, 2, \cdots, n\}$ as a collection of agents within a phase space $(\mathcal{X}, T)$ such that all agents within the flock interact with their nearest neighbors in a topological sense so as to preserve heading cohesion.*

Every agent within a flock has similar dynamics to that of its neighbor(s). Furthermore, agents travel at the same linear speed, v; the angular headings, w, however, may be different between agents. The state of a single agent i within a flock will be defined as $\boldsymbol{x}^{(i)}$. Motion within a flock is described as a leaderless coordination of its n autonomous agents. Each agent's continuous-time dynamics evolves as

$$\dot{\boldsymbol{x}}^{(i)}(t) = \begin{bmatrix} \dot{\boldsymbol{x}}_1^{(i)}(t) \\ \dot{\boldsymbol{x}}_2^{(i)}(t) \\ \dot{\boldsymbol{x}}_3^{(i)}(t) \end{bmatrix} = \begin{bmatrix} v(t) \cos \boldsymbol{x}_3^{(i)}(t) \\ v(t) \sin \boldsymbol{x}_3^{(i)}(t) \\ \langle w^{(i)}(t) \rangle_r \end{bmatrix}, \text{ where } \langle w^{(i)}(t) \rangle_r = \frac{w_i(t) + \sum_{j \in \mathcal{N}_i(t)} w_j(t)}{1 + N_i(t)}, \tag{13}$$

for agents $i = \{1, 2, 3, ..., n\}$, where t is the continuous-time index, $\boldsymbol{x}$ denotes points in $\mathbb{R}^n$, and $w^{(i)}(t)_r$ is the average orientation of agent i w.r.t its neighbors is $\langle w^{(i)}(t) \rangle_r$.

Definition 2 (Payoff of a Flock). *To every agent i within a flock, F, with finite number of agents N, we associate a payoff, $\boldsymbol{V}(\boldsymbol{x}^{(i)})$, that encodes the outcome of its topological interaction with its neighbors.*

Definition 3 (Definition 5.7, [25]). *We consider the heading goal for a local group F_j[7] within a murmuration of flocks F as an N-person differential game with a target set $\mathcal{L}_0^j$. The strategy N-tuple is said to be playable at $(\boldsymbol{x}_0, t_0)$ if it generates a trajectory $\xi(\cdot)$ such that $(\boldsymbol{x}(t), t) \in \mathcal{L}_0^j$ for finite t. Such a trajectory $\xi(\cdot)$ is said to be terminating.*

As mentioned in the introduction, we cannot solve the initial value problem in a classical way on $\mathbb{R}^n \times [T, 0]$ in general. Viscosity solutions provide a particular means of finding a unique solution with a clear interpretation in terms of the generalized optimal control problem, even in the presence of stochastic perturbations.

Each agent within a flock interacts with a fixed number of neighbors, n_c, within a fixed topological range, r_c. This topological range is consistent with findings in collective swarm behaviors and it reinforces *group cohesion* [11]. However, we are interested in *robust group cohesion* in reachability analysis. Therefore, we let a pursuer, $\boldsymbol{P}$, with a worst-possible disturbance attack the flock, and we take it that flocks of agents constitute an evading player, $\boldsymbol{E}$.

Returning to (13), for a single flock, we now provide a sketch for the HJI formulation for a heading consensus problem.

---

[7] The subscript j of F is used to identify a distinct flock of agents within a murmuration on a state space.

4.1   Framework for Separated Payoffs

We now make the following abstractions to enable our problem formulation. A murmuration's global heading is predetermined and each agent i within each flock, F_j, ($j = 1, \cdots, n$) in the murmuration has a constant linear velocity, v^i. An agent's orientation is its control input, given by the average of its own orientation and that of its neighbors. Instead of metric distance interaction rules that make agents very vulnerable to predators [11], we resort to a topological interaction rule[8].

4.2   Nearest Neighbors Computation

What constitutes an agent's neighbors are computed based on empirical findings and studies from the lateral vision of birds and fishes [11, 14, 26]. This lateral vision governs their anisotropic kinematic density and structure. Importantly, starlings' lateral visual axes and their lack of a rear sector reinforces their lack of nearest neighbors in the front-rear direction. As such, this enables them to maintain a tight density and robust heading during formation and flight.

Definition 4 (Neighbors of an Agent). *We define the neighbors of agent i in flock F_j at time t as the set of all agents that lie within a predefined radius, r_n, of agent i. In every iteration of the game, we update an agent's neighbors as delineated in Algorithm 1.*

   The algorithm for computing the nearest neighbors is given in Algorithm 1. On lines 3 and 7 of Algorithm 1, cohesion is reinforced by leveraging the observations above. Each agent within a flock F_j interacts with a fixed number of neighbors, n_c, within a fixed topological range, r_c. This topological range is consistent with findings in collective swarm behaviors and it reinforces *group cohesion* [11]. However, we are interested in *robust group cohesion* in reachability analysis. Therefore, we let a pursuer, $\boldsymbol{P}$, with a worst-possible disturbance attack the flock, and we take it that flocks of agents constitute an evading player, $\boldsymbol{E}$.

4.3   Global Isotropy via Local Anisotropy

It has been observed that structural anisotropy is not merely an effect of a preferential velocity in animal flocking kinematics but rather an explicit effect of the anisotropic interaction character itself.

   A distinct idea is that the mutual position chosen by the animals is the one that maximizes the sensitivity to changes of heading and speed of their neighbors (9). According to this hypothesis, even though vision is the main mechanism of interaction, optimization determines the anisotropy of neighbors, and not the eye's structure. There is also the possibility that each individual keeps the front neighbor at larger distances to avoid collisions. This collision avoidance mechanism is vision-based but not related to the eye's structure.

---

[8] With metric distance rules, we will have to formulate the breaking apart of value functions that encode a consensus heading problem in order to resolve the extrema of multiple payoffs; which is typically what we want to mitigate against during real-world autonomous tasks.

Algorithm 1 Nearest Neighbors For Agents in a Flock.

1: Given a set of agents $\boldsymbol{a} = \{a_1, a_2, \cdots, a_{n_a} \,|\, [a] = n_a\}$ ▷ n_a agents in a flock F_k.
2: **function** UPDATENEIGHBOR(n)
3:     **for** i in $1, \ldots, n$ **do**   ▷ Look to the right and update neighbors.
4:         **for** j in $i + 1, \ldots, n$ **do**
5:             COMPARE_NEIGHBOR($a[i]$, $a[j]$)
6:         **end for**
7:         **for** j in $i - 1$ down to 0 **do**   ▷ Look to the left and update neighbors.
8:             COMPARE_NEIGHBOR($a[i]$, $a[j]$)
9:         **end for**
10:     **end for**
11:     **for** each $a_i \in F_k$, $i = 1, \cdots n_a$ **do**   ▷ Recursively update agents' headings.
12:         Update headings according to (13).
13:     **end for**
14: **end function**

1: **function** COMPARE_NEIGHBOR(a_1, a_2)   ▷ (a_1, a_2): distinct instances of AGENT.
2:     **if** $|a_1.\text{label} - a_2.\text{label}| < a_1.r_c^1$ ▷ r_c^n: agent n's capture radius.
3:         a_1.UPDATE_NEIGHBORS(a_2) **then**
4:     **end if**
5: **end function**

1: **procedure** AGENT(a_i, Neighbors={}) ▷ Neighbors: Set of neighbors of this agent.
2:             ▷ Agent a_i with attributes label $\in \mathbb{N}$, avoid and capture radii, r_a, r_c.
3:     **function** UPDATE_NEIGHBORS(neigh)
4:         **if** length(neigh)> 1 **then**   ▷ Multiple neighbors.
5:             **for** each neighbor of neigh **do**
6:                 UPDATE_NEIGHBORS(neighbor)   ▷ Recursive updates.
7:             **end for**
8:         **end if**
9:         Add neigh to Neighbors
10:     **end function**
11: **end procedure**

Because of the robust group cohesion philosophy, we take it that every agent within a flock $flock_j$, under attack is in relative coordinates with a pursuer, $\boldsymbol{P}^j$. By averaging the heading of individual agents orientations with that of its neighborsc.f. (13), individual agents within a flock can achieve instantaneous response to danger when a pursuer is nearby. TO-DO: In this specialized case, capture does not necessarily occur, because the $\boldsymbol{E}$ and $\boldsymbol{P}$'s speeds and maximum turn radius are equal: if both players start the game with the same initial velocity and orientation, the relative equations of motion show that $\boldsymbol{E}$ can mimic $\boldsymbol{P}$'s strategy by forever keeping the starting radial separation [20]. As such, the *barrier* is closed and the *game of kind* is to determine the surface. However, owing to the high-dimensionality of the state space, we cannot resolve this barrier analytically, hence we resort to numerical approximation methods – in particular, we leverage a parallel Lax-Friedrichs integration scheme [27] which we implement in Cupy [28] in
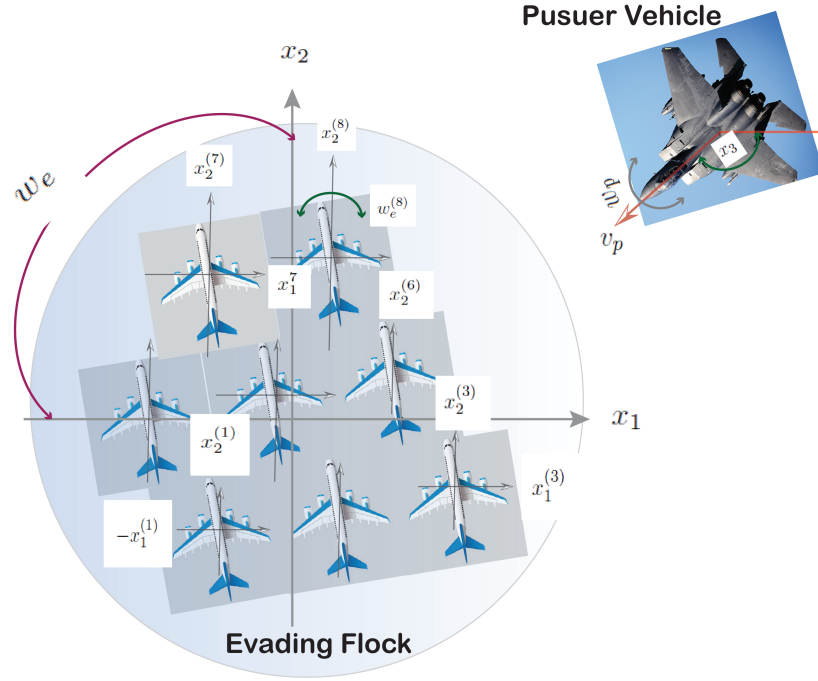
Fig. 3: Illustration of robust heading consensus for a flock. Each agent within the Evading player's control are in relative coordinates w.r.t a pursuing adversary. Each agent (identified by index i) within the evading flock is parameterized by three state components: the linear velocities $(\boldsymbol{x}_1^{(i)}, \boldsymbol{x}_2^{(i)})$, and heading $w^{(i)}$. When we need to distinguish an agent within a flock from another flock, we shall use the index of the flock e.g. j as a subscript for a particular e.g. $\boldsymbol{x}_1^{(i)_j}$.

order to provide a *consistent* and *monotone* solution to the Hamiltonians of these HJI equations[9].

Therefore, for an agent i within a flock with index j in a murmuration, the equations of motion under attack from a predator (see Fig. 3) is

$$
\begin{bmatrix}
\dot{\boldsymbol{x}}_1^{(i)_j}(t) \\
\dot{\boldsymbol{x}}_2^{(i)_j}(t) \\
\dot{\boldsymbol{x}}_3^{(i)_j}(t)
\end{bmatrix}
=
\begin{bmatrix}
-v_e^{(i)_j}(t) + v_p^{(j)} \cos \boldsymbol{x}_3^{(i)_j}(t) + \langle w_e^{(i)_j} \rangle_r \boldsymbol{x}_2^{(i)_j}(t) \\
v_p^{(i)_j}(t) \sin \boldsymbol{x}_3^{(i)_j}(t) - \langle w_e^{(i)_j} \rangle_r \boldsymbol{x}_1^{(i)_j}(t) \\
w_p^{(j)}(t) - \langle w_e^{(i)_j}(t) \rangle_r
\end{bmatrix}
\text{ for } i = 1, \cdots, N
$$
(14)

---

[9] Consistent solutions to HJ equations are those whose explicit marching schemes via discrete approximations to the HJ IVP agree with the nonlinear HJ solution [4]. Such schemes are said to be *monotone* e.g. on $[-\mathbb{R}, \mathbb{R}]$ if the numerical approximation to the vector field of interest is a nondecreasing function of each argument of the discrete approximation to the vector field.

where N is the number of flocks. Read $\boldsymbol{x}_1^{(i)_j}(t)$: the first component of the state of an agent i at time t which belongs to the flock j in the murmuration. As mentioned in Section 2, the evading player at anytime has controls $\{\boldsymbol{u}^1, \boldsymbol{u}^2, \cdots \boldsymbol{u}^n\}$ for agents $i = 1, \cdots, n$ completely under its will. Solving for such complex backward reach-avoid tube is akin to splitting the state space into a number of parts separated by surfaces. We assume that the *value* of a flock heading control (differential game) exists, so that the terminal value function is

$$\frac{\partial \boldsymbol{V}_j^-}{\partial t} + \boldsymbol{H}_j^-(t; \boldsymbol{x}, \boldsymbol{u}, \boldsymbol{v}, \boldsymbol{V}_{\boldsymbol{x}_j}^-) = 0, \ t \in [0, T] \ \boldsymbol{x} \in \mathbb{R}^n \tag{15a}$$

$$\boldsymbol{V}_j^-(\boldsymbol{x}, T) = g_j(x(T)), \quad \boldsymbol{x} \in \mathbb{R}^m, \quad j = 1, \cdots, n \tag{15b}$$

with lower Hamiltonian,

$$\boldsymbol{H}_j^-(t; \boldsymbol{x}, \boldsymbol{u}, \boldsymbol{v}, p) = \max_{u \in \mathcal{U}} \min_{v \in \mathcal{V}} \langle f_j(t; \boldsymbol{x}, \boldsymbol{u}, \boldsymbol{v}), p_j \rangle, \quad j = 1, \cdots, n, \tag{16}$$

where n is the total number of separate and distinct flocks on a state space. We follow [19]'s definition by ascribing to these surfaces the term *singular surfaces*, which signifies $(n-1)$-manifolds in n-space. On the respective surfaces, we are concerned with the resolution of the respective *values* i.e. $\{\boldsymbol{V}_1, \cdots, \boldsymbol{V}_n\}$ for distinct flocks $\{F_1, F_2, \cdots, F_n\}$ on the distinct surfaces of the state spaces $\{\mathcal{X}_1, \mathcal{X}_2, \cdots, \mathcal{X}_n\}$. The reader should note that $\mathcal{X} = \mathcal{X}_1 \cup \mathcal{X}_2 \cup \cdots \cup \mathcal{X}_n$. Similarly, we attribute the term *in the small* to determine the smooth parts of the singular surface solution, and when they are stitched together into the total solution, we shall describe them as *in the large*.

To encourage robust cohesion, a pursuer can attack any flock or a group of flocks within the murmuration from two distinct surfaces, which we call a $\boldsymbol{P}$ or an $\boldsymbol{E}$ direction. We call the side of the surface reached after penetration in the $\boldsymbol{P} - [\boldsymbol{E}-]$ direction the $\boldsymbol{P} - [\boldsymbol{E}]$ *side*. There exists at least one value $\bar{\alpha}$ of α such that if $\alpha = \bar{\alpha}$, no vector in the β-vectogram[10] penetrates the surface in the E-direction. Similar arguments can be made for $\bar{\beta}$ which prevents penetration in the P-direction. We adopt [19]'s terminology and call these surfaces semi-permeable surfaces (SPS).

We are dealing with a family of games based on different starting points for local flocks that on the whole constitute a murmuration; therefore, we construct the respective target sets for each individual agent implicitly on the state space as $\boldsymbol{V} : [-T, 0] \times \mathcal{X} \to \mathbb{R}$. In starlings, agents move in local flocks of six to seven nearest neighbors [11] in order to preserve cohesion and heading consensus. Therefore, we define the target set and the tube as

$$\mathcal{L}_0 = \left\{ \boldsymbol{x} \in \bar{\Omega} | \boldsymbol{V}(\boldsymbol{x}, 0) \leq 0 \right\}, \tag{17}$$

$$\mathcal{L}([\tau, 0], \mathcal{L}_0) = \left\{ \boldsymbol{x} \in \bar{\Omega} | \boldsymbol{V}(\boldsymbol{x}, \tau) \leq 0 \right\} \tag{18}$$

where $\tau \in [-T, 0]$.

Throughout the game, we assume that the roles of $\boldsymbol{P}$ and $\boldsymbol{E}$ do not change, so that when capture can occur, a necessary condition to be satisfied by the saddle-point controls

---

[10] A $\beta-$vectogram is the resulting state space when a the strategy β is applied in computing the optimal control law for an agent.

of the players is the Hamiltonian. For a flock, j, this is the total energy exerted by each agent i in the flock so that we can write the total Hamiltonian of a murmuration as

$$\boldsymbol{H}(\boldsymbol{x}, p) = \sum_{j=1}^{N_f} \sum_{i=1}^{N_a} H_j^{(i)}(\boldsymbol{x}, p) \tag{19}$$

where N_f is the total number of distinct flocks in a murmuration, N_a is the total number of agents within flock j. $H_j^{(i)}(\boldsymbol{x}, p)$ is the Hamiltonian of flock j, given by

$$H_j^{(i)}(\boldsymbol{x}, p) = -\left(\max_{w_e^{(i)_j} \in [\underline{w}_e^j, \bar{w}_e^j]} \min_{w_p^{(i)_j} \in [\underline{w}_p^j, \bar{w}_p^j]} \left[p_1^{(i)_j}(t)\, p_2^{(i)_j}(t)\, p_3^{(i)_j}(t) \right] \right.$$
$$\left. \begin{bmatrix} -v_e^{(i)_j}(t) + v_p^{(j)} \cos \boldsymbol{x}_3^{(i)_j}(t) + \langle w_e^{(i)_j} \rangle_r(t) \boldsymbol{x}_2^{(i)_j}(t) \\ v_p^j(t) \sin \boldsymbol{x}_3^{(i)_j}(t) - \langle w_e^{(i)_j} \rangle_r(t) \boldsymbol{x}_1^{(i)_j}(t) \\ w_p^j(t) - \langle w_e^{(i)_j}(t) \rangle_r \end{bmatrix} \right), \tag{20}$$

where $w_e^{(i)_j}$ is the heading of an evader i within a flock j and $w_p^{(j)}$ is the heading of a pursuer aimed at flock j; $\underline{w}_e^{(i)_j}$ is the orientation that corresponds to the orientation of the agent with minimum turn radius among all the neighbors of agent i, inclusive of agent i at time t; similarly, $\bar{w}_e^{(i)_j}$ is the maximum orientation among all of the orientation of agent i's neighbors. For the pursuer, its minimum and maximum turn rates are fixed so that we have $\underline{w}_p^j$ as the minimum turn bound of the pursuing vehicle, and $\bar{w}_p^j$ is the maximum turn bound of the pursuing vehicle. Henceforth, we drop the templated time arguments for ease of readability. Rewriting (20), we find $\boldsymbol{H}_j^{(i)}(\boldsymbol{x}, p)$ as

$$\boldsymbol{H}_j^{(i)}(\boldsymbol{x}, p) = -\left(\max_{w_e^{(i)_j} \in [\underline{w}_e^j, \bar{w}_e^j]} \min_{w_p^{(i)_j} \in [\underline{w}_p^j, \bar{w}_p^j]} \left[-p_1^{(i)_j} v_e^{(i)_j} + p_1^{(i)_j} v_p^j \cos \boldsymbol{x}_3^{(i)_j} \right. \right.$$
$$\left. \left. + p_1^{(i)_j} \langle w_e^{(i)_j} \rangle_r \boldsymbol{x}_2^{(i)_j} + p_2^{(i)_j} v_p^j \sin \boldsymbol{x}_3^{(i)_j} - p_2^{(i)_j} \langle w_e^{(i)_j} \rangle_r \boldsymbol{x}_1^{(i)_j} + p_3^{(i)_j} \left(w_p^j - \langle w_e^{(i)} \rangle_r \right) \right] \right),$$
$$= p_1^{(i)_j} \left(v_e^{(i)_j} - v_p^j \cos \boldsymbol{x}_3^{(i)_j} \right) - p_2^{(i)_j} v_p^j \sin \boldsymbol{x}_3^{(i)_j}$$
$$+ \left(\max_{w_e^{(i)_j} \in [\underline{w}_e^j, \bar{w}_e^j]} \min_{w_p^{(i)_j} \in [\underline{w}_p^j, \bar{w}_p^j]} \begin{bmatrix} \langle w_e^{(i)_j} \rangle_r \left(p_2^{(i)_j} \boldsymbol{x}_1^{(i)_j} - p_1^{(i)_j} \boldsymbol{x}_2^{(i)_j} \right) \\ -p_3^{(i)_j} \left(w_p^j - \langle w_e^{(i)} \rangle_r \right) \end{bmatrix} \right). \tag{21}$$

In this work, we consider the special case where the linear speeds of the evaders and pursuer are equal i.e. $v_e = v_p = +1$. Then the Hamiltonian $\boldsymbol{H}_j^{(i)}(\boldsymbol{x}, p)$ in (21) becomes

$$\boldsymbol{H}_j^{(i)}(\boldsymbol{x}, p) = p_1^{(i)_j} \left(1 - \cos \boldsymbol{x}_3^{(i)_j} \right) - p_2^{(i)_j} \sin \boldsymbol{x}_3^{(i)_j} - \underline{w}_p^j \left| p_3^{(i)_j} \right|$$
$$+ \bar{w}_e^j \left| \left(p_2^{(i)_j} \boldsymbol{x}_1^{(i)_j} - p_1^{(i)_j} \boldsymbol{x}_2^{(i)_j} + p_3^{(i)_j} \right) \right|. \tag{22}$$

From (19), we thus write

$$
\boldsymbol{H}(\boldsymbol{x}, p) = \sum_{j=1}^{N_f} \sum_{i=1}^{N_a} p_1^{(i)} \left(1 - \cos \boldsymbol{x}_3^{(i)_j} \right) - p_2^{(i)_j} \sin \boldsymbol{x}_3^{(i)_j} - \underline{w}_p^j \left| p_3^{(i)_j} \right|
$$

$$
+ \bar{w}_e^j \left| p_2^{(i)_j} \boldsymbol{x}_1^{(i)_j} - p_1^{(i)_j} \boldsymbol{x}_2^{(i)_j} + p_3^{(i)_j} \right|. \tag{23}
$$

5 Experiments

In all our experiments, robust cohesion and anisotropy is reinforced by having one player be a pursuer against a flock of evaders as seen in Fig. 3. We initialize each flock's agents to distinct positions on the vectogram. All agents share the same linear speed, v but varying orientations $\langle w^{(i)}(t) \rangle_r$ that are averaged across every nearest neighbor in a flock according to (13). Nearest neighbors are updated according to Algorithm 1.

5.1 Interagents Spatial Structure

- put reference bird at origin; then randomly initialize other birds with a random walk in the state space with a covariance of .5 [?]
- we randomly initialized covariance in random walker at start
- every local flock has its own value function governed by a target set
- every bird is spatially correlated on a large grid that parameterizes a flock

- we initialize the flock's state coverage as follows
- the evader (or reference vehicle) holds has a state space that spans the following intervals on the x, y, z state plane $[x_1^-, x_1^+, x_2^-, x_2^+, x_3^-, x_3^+]$
- every follower vehicle in the flock has its state space coverage specified as $[x_1^- - \epsilon, x_1^+ - \epsilon, x_2^- - \epsilon, x_2^+, x_3^- - \epsilon, x_3^+ - \epsilon]$
- we find that this initialization helps the agents maintain good coverage on the entire state space: it easily provides bounds, a nice spatial distribution of flight coverage. For instance, if all flocks are positioned at the origin of their grids, then what we have is a single line of leader vs multiple followers that achieves
- every flock has its own payoff, which are related to that of nearest neighbor interacting flocks via dispersal or X surfaces/lines/or hyperplanes.

6 Conclusion.

References

1. Osher, S., Shu, C.W.: High-Order Essentially Nonoscillatory Schemes for Rotary-Wing Wake Computations. Journal of Aircraft **41**(2), 258–267 (2004). DOI 10.2514/1.9320 1
2. Crandall, M.G., Majda, A.: Monotone difference approximations for scalar conservation laws. Mathematics of Computation **34**(149), 1–21 (1980) 1

3. Evans, L., Souganidis, P.E.: Differential games and representation formulas for solutions of Hamilton-Jacobi-Isaacs equations. Indiana Univ. Math. J **33**(5), 773–797 (1984) 1, 6, 7

4. Crandall, M.G., Lions, P.L.: Two Approximations of Solutions of Hamilton-Jacobi Equations. Mathematics of Computation **43**(167), 1 (1984) 2, 12

5. Herbert, S., Choi, J.J., Sanjeev, S., Gibson, M., Sreenath, K., Tomlin, C.J.: Scalable learning of safety guarantees for autonomous systems using hamilton-jacobi reachability. arXiv preprint arXiv:2101.05916 (2021) 2, 3, 8

6. Bansal, S., Chen, M., Herbert, S., Tomlin, C.J.: Hamilton-Jacobi Reachability: A Brief Overview and Recent Advances. 2017 IEEE 56th Annual Conference on Decision and Control, ACC 2017 pp. 2242–2253 (2018) 2

7. Bajcsy, A., Bansal, S., Bronstein, E., Tolani, V., Tomlin, C.J.: An Efficient Reachability-based Framework for Provably Safe Autonomous Navigation in Unknown Environments. In: 2019 IEEE 58th Conference on Decision and Control (CDC), pp. 1758–1765. IEEE (2019) 2, 3

8. Bellman, R.: Dynamic programming. Princeton University Press (1957) 2

9. Mitchell, I.: A Robust Controlled Backward Reach Tube with (Almost) Analytic Solution for Two Dubins Cars. EPiC Series in Computing **74**, 242–258 (2020) 3

10. Mitchell, I.M., Bayen, A.M., Tomlin, C.J.: A time-dependent Hamilton-Jacobi formulation of reachable sets for continuous dynamic games. IEEE Transactions on Automatic Control **50**(7), 947–957 (2005). DOI 10.1109/TAC.2005.851439 3, 5, 7

11. Ballerini, M., Cabibbo, N., Candelier, R., Cavagna, A., Cisbani, E., Giardina, I., Lecomte, V., Orlandi, A., Parisi, G., Procaccini, A., Viale, M., Zdravkovic, V.: Interaction ruling animal collective behavior depends on topological rather than metric distance: Evidence from a field study. Proceedings of the National Academy of Sciences **105**(4), 1232–1237 (2008). DOI 10.1073/pnas.0711437105. URL https://www.pnas.org/content/105/4/1232 3, 8, 9, 10, 13

12. Cavagna, A., Cimarelli, A., Giardina, I., Parisi, G., Santagati, R., Stefanini, F., Viale, M.: Scale-free correlations in starling flocks. Proceedings of the National Academy of Sciences **107**(26), 11,865–11,870 (2010) 3

13. Bialek, W., Cavagna, A., Giardina, I., Mora, T., Silvestri, E., Viale, M., Walczak, A.M.: Statistical mechanics for natural flocks of birds. Proceedings of the National Academy of Sciences **109**(13), 4786–4791 (2012) 3

14. Jadbabaie, A., Lin, J., Morse, A.S.: Coordination of groups of mobile autonomous agents using nearest neighbor rules. IEEE Transactions on automatic control **48**(6), 988–1001 (2003) 3, 4, 10

15. Haiken, M.: These birds flock in mesmerizing swarms of thousandsbut why is still a mystery. (2021). URL https://www.nationalgeographic.com/animals/article/these-birds-flock-in-mesmerizing-swarms-why-is-still-a-mystery 3

16. Crandall, M.G., Lions, P.L.: Viscosity solutions of hamilton-jacobi equations. Transactions of the American mathematical society **277**(1), 1–42 (1983) 3, 6

17. Lygeros, J.: On reachability and minimum cost optimal control. Automatica **40**(6), 917–927 (2004) 3

18. Chen, M., Herbert, S.L., Vashishtha, M.S., Bansal, S., Tomlin, C.J.: Decomposition of Reachable Sets and Tubes for a Class of Nonlinear Systems. IEEE Transactions on Automatic Control **63**(11), 3675–3688 (2018). DOI 10.1109/TAC.2018.2797194 3, 8

19. Isaacs, R.: Differential games 1965. Kreiger, Huntigton, NY 5, 8, 13

20. Merz, A.: The game of two identical cars. Journal of Optimization Theory and Applications **9**(5), 324–343 (1972) 5, 11

21. Dubins, L.E.: On curves of minimal length with a constraint on average curvature, and with prescribed initial and terminal positions and tangents. American Journal of mathematics **79**(3), 497–516 (1957) 5

22. Zhou, K., Doyle, J.C.: Essentials of Robust Control, vol. 104. Prentice hall Upper Saddle River, NJ (1998) 5
23. Evans, L., Souganidis, P.E.: Differential games and representation formulas for solutions of Hamilton-Jacobi-Isaacs equations. Indiana Univ. Math. J **33**(5), 773–797 (1984) 6, 7
24. Bansal, S., Tomlin, C.J.: DeepReach : A Deep Learning Approach to High-Dimensional Reachability 8
25. Basar, T., Olsder, G.J.: Dynamic noncooperative game theory, vol. 23. Siam (1999) 9
26. Helbing, D., Farkas, I., Vicsek, T.: Simulating dynamical features of escape panic. Nature **407**(6803), 487–490 (2000) 10
27. Crandall, M.G., Evans, L.C., Lions, P.L.: Some Properties of Viscosity Solutions of Hamilton-Jacobi Equations. Transactions of the American Mathematical Society **282**(2), 487 (1984). DOI 10.2307/1999247 11
28. Nishino, R., Loomis, C., Hido, S.: Cupy: A numpy-compatible library for nvidia gpu calculations. 31st confernce on neural information processing systems **151** (2017) 11
29. Vicsek, T., Czirók, A., Ben-Jacob, E., Cohen, I., Shochet, O.: Novel type of phase transition in a system of self-driven particles. Physical review letters **75**(6), 1226 (1995)